Astronomy & Astrophysics

Alleviating α quenching by solar wind and meridional flows

D. Mitra[1], D. Moss[2], R. Tavakol[3], and A. Brandenburg[1,4]

[1] NORDITA, AlbaNova University Center, Roslagstullsbacken 23, 10691 Stockholm, Sweden
   e-mail: dhruba.mitra@gmail.com
[2] School of Mathematics, University of Manchester, Oxford Road, Manchester M13 9PL, UK
[3] Astronomy Unit, School of Mathematical Sciences, Queen Mary University of London, Mile End Road, London E1 4NS, UK
[4] Department of Astronomy, Stockholm University, 10691 Stockholm, Sweden

ABSTRACT

Aims. We study the ability of magnetic helicity expulsion to alleviate catastrophic α-quenching in mean field dynamos in two–dimensional spherical wedge domains.
Methods. Motivated by the physical state of the outer regions of the Sun, we consider $\alpha^2\Omega$ mean field models with a dynamical α quenching. We include two mechanisms which have the potential to facilitate helicity expulsion, namely advection by a mean flow ("solar wind") and meridional circulation.
Results. We find that a wind alone can prevent catastrophic quenching, with the field saturating at finite amplitude. In certain parameter ranges, the presence of a large-scale meridional circulation can reinforce this alleviation. However, the saturated field strengths are typically below the equipartition field strength. We discuss possible mechanisms that might increase the saturated field.

Key words. Sun: dynamo – magnetohydrodynamics (MHD)

1. Introduction

Mean field dynamo models have provided an important framework for studying the generation of large-scale astrophysical magnetic fields and their spatio-temporal dynamics. However, these widely used models have been presented with a serious challenge – namely the so called catastrophic α quenching (Gruzinov & Diamond 1994). In the mean field (MF) context this effect, which is a consequence of the conservation of magnetic helicity (Krause & Rädler 1980; Zeldovich et al. 1983), manifests itself as the decrease of the α-effect with increasing magnetic Reynolds number Re_M (Vainshtein & Cattaneo 1992; Cattaneo & Hughes 1996) at finite field strength. In models without magnetic helicity fluxes, the quenching of α can become severe, with α decreasing as Re_M^{-1} – truly catastrophic for dynamo action in the Sun, stars and galaxies where the Reynolds numbers are all very large ($>10^9$). This catastrophic quenching is captured by mean-field models which use dynamical alpha quenching, such as that considered by Blackman & Brandenburg (2002). This catastrophic quenching is independent of the details of the dynamo mechanism and is a direct effect of the conservation of magnetic helicity. See, e.g., Brandenburg & Käpylä (2007) who have demonstrated catastrophic quenching for non-local alpha effect or Chatterjee et al. (2011) who have demonstrated the occurrence of catastrophic quenching in distributed dynamos. It has been suggested that the quenching may be alleviated by the expulsion of magnetic helicity through open boundaries (Blackman & Field 2000; Kleeorin et al. 2000). At least three different physical mechanisms may help in the expulsion of small scale magnetic helicity: (a) large scale shear (Vishniac & Cho 2001; Subramanian & Brandenburg 2004; Brandenburg & Sandin 2004; Moss & Sokoloff 2011); (b) turbulent diffusion of magnetic helicity (Mitra et al. 2010a); (c) non-zero mean flow out from a boundary of the domain, e.g. a wind. A number of

recent studies have demonstrated the possibility of this alleviation of quenching for solar (Chatterjee et al. 2010, 2011; Guerrero et al. 2010) and galactic dynamos (e.g. Shukurov et al. 2006).

In this paper we study the effects of a number of mechanisms which may facilitate the expulsion of magnetic helicity from the dynamo region. Initially we consider the effects of advection by a mean flow in a similar manner to Shukurov et al. (2006); see also the recent study in a one dimensional model by Brandenburg et al. (2009). We envisage that in the Sun the wind could be loaded with magnetic helicity through coronal mass ejections (Blackman & Brandenburg 2003). Another potentially important mechanism is meridional circulation. The presence of such a circulation in the Sun is supported by a number of observations which have found evidence for a near-surface poleward flow of 10–20 ms^{-1}. Even though the corresponding compensating equatorward flow has not yet been detected, it is however assumed it must exist because of mass conservation. Substantial effort has recently gone into the construction of flux transport dynamo models which differ from the usual $\alpha\Omega$ dynamos by including an additional advective transport of magnetic flux by meridional circulation. (see e.g. Dikpati & Gilman 2009, for a recent summary). If magnetic flux is advected by meridional circulation, it can be expected that such a circulation will also transport magnetic helicity to the surface layers, which might thus facilitate its subsequent expulsion by the wind. We therefore study the effects of meridional circulation on the quenching.

The structure of the paper is as follows. In Sect. 2 we introduce our model and its various ingredients. Section 3 contains our results, and we give a short summary here. First we consider our model with an imposed wind but no meridional circulation. We show that a strong enough wind that penetrates deeply enough into the convection zone can indeed alleviate quenching. We then make a systematic study of the alleviation of quenching

as a function of the two parameters specifying the wind, namely the maximum velocity and the depth down to which the wind penetrates the convection zone. Next we select a particular set of these two parameters such that for large Re_M there is no alleviation of quenching. We then introduce a meridional circulation and show that a combination of a wind and circulation is able to limit the quenching in cases where the wind alone cannot. We further study the effect of the characteristic velocity of meridional circulation on quenching. Our conclusions are presented in Sect. 4.

2. The model

We study two-dimensional (axisymmetric) mean field models in a spherical wedge domain, $r_1 \leq r \leq r_2$, $\theta_1 \leq \theta \leq \pi/2$, where r, θ, ϕ are spherical polar coordinates. The choice of this "wedge" shaped domain is motivated by recent Direct Numerical Simulations (DNSs) of forced and convective dynamos in spherical wedges cut from spheres (Mitra et al. 2010b; Käpylä et al. 2010), and the intention to make a similar development of this work.

We consider an $\alpha^2\Omega$ mean field model with a "dynamical alpha" in the presence of an additional mean flow $\overline{U}$. In the simplest case, where we consider no wind and no meridional circulation, the mean flow is in the form of a uniform rotational shear given by $\overline{U} = U^{\text{shear}} = \hat{\phi}S(r - r_0)\sin\theta$. For the more realistic cases we use

$$\overline{U} = U^{\text{shear}} + U^{\text{wind}} + U^{\text{circ}}, \tag{1}$$

where U^{wind} and U^{circ} are respectively the large-scale velocity of the wind and circulation. The particular forms we use are given in Sects. 2.1 and 2.2 below. Thus, we integrate

$$\partial_t \overline{B} = \nabla \times (\overline{U} \times \overline{B} + \overline{\mathcal{E}}) + \eta\nabla^2\overline{B}, \tag{2}$$

$$\partial_t \alpha_M = -2\eta k_f^2\left(\frac{\overline{\mathcal{E}} \cdot \overline{B}}{B_{\text{eq}}^2} + \frac{\alpha_M}{Re_M}\right) - \nabla \cdot (\alpha_M \overline{U}), \tag{3}$$

where $\overline{\mathcal{E}} = \alpha\overline{B} - \eta_t\overline{J}$, and $\alpha = \alpha_M + \alpha_K$ is the sum of the magnetic and kinetic α-effects respectively. The magnetic Reynolds number, $Re_M/3 \equiv \eta_t/\eta$ and B_{eq} is the equipartition field strength. We take $\eta_t = 1$, $B_{\text{eq}} = 1$ and $k_f = 100$ in our simulations. Here Eq. (2) is the standard induction equation for mean field models and Eq. (3) describes the dynamical evolution of α; see Blackman & Brandenburg (2002). The last term in the right hand side of Eq. (3) models the advective flux of magnetic helicity.

We solve Eqs. (2) and (3) using the PENCIL CODE[1] which employs a sixth order centered finite-difference method to evaluate the spatial derivatives and a third order Runge-Kutta scheme for time evolution.

Our aim here is to study the effects of the various mechanisms discussed above in alleviating the catastrophic quenching of the magnetic field as Re_M increases.

2.1. The wind and the "corona"

In order to include the effects of the solar wind we must include an outer region in our model through which the wind flows, by extending the outer boundary beyond the convection zone to radius $r_3 > r_2$. We shall refer to the region $r_2 \leq r \leq r_3$ as the "corona". We take the wind to be strong in the corona and to

---

[1] http://pencil-code.googlecode.com/

grow weaker as we go into the convection zone. This is represented by choosing the following form for U^{wind},

$$U_r^{\text{wind}} = \frac{1}{2}U_0\left[1 + \tanh\left(\frac{r - r_2}{w}\right)\right], \tag{4}$$

$$U_\theta^{\text{wind}} = 0, \tag{5}$$

$$U_\phi^{\text{wind}} = 0, \tag{6}$$

where U_0 and w are control parameters which determine the strength of the wind speed and its depth of penetration into the convection zone respectively. Larger values of w correspond to deeper penetration. We let the kinematic α-effect to go to zero in the corona by choosing

$$\alpha_K = -\frac{\alpha_0}{2}\tanh\left(\frac{\theta - \pi/2}{0.05}\right)\left[1 - \tanh\left(\frac{r - r_2}{w_\alpha}\right)\right], \tag{7}$$

with $\alpha_0 = 16$.

2.2. The meridional circulation

We consider the effects of a meridional circulation, by including a velocity U^{circ} given by

$$U_r^{\text{circ}} = v_{\text{amp}}g(r)\frac{1}{\sin\theta}\frac{\partial}{\partial\theta}(\sin\theta\,\psi), \tag{8}$$

$$U_\theta^{\text{circ}} = -v_{\text{amp}}g(r)\frac{1}{r}\frac{\partial}{\partial r}(r\psi), \tag{9}$$

$$\psi = \frac{f(r)}{r}\sin^2(\theta - \theta_1)\cot\theta, \tag{10}$$

$$f(r) = (r - r_2)(r - r_1)^2, \tag{11}$$

$$g(r) = \frac{1}{2}\left[1 - \tanh\left(\frac{r - r_2}{w_{\text{circ}}}\right)\right], \tag{12}$$

$$U_\phi^{\text{circ}} = 0. \tag{13}$$

Here v_{amp} is a parameter controlling the magnitude of circulation speed and w_{circ} determines the effective depth of penetration of the circulation into $r > r_2$. As a characteristic speed of circulation, v_{circ}, we take the maximum absolute magnitude of the θ component of U^{circ} at $r = r_2$, i.e. at the surface of the Sun. Helioseismology shows this velocity to be about 10 to 20 metres per second in the Sun. A typical velocity field is shown in Fig. 1, and the profile of α_K is shown in Fig. 2. In these figures, the parameters are chosen to be $\alpha_0 = 16$, $w_\alpha = 0.2$, $U_0 = 2$, $r_2 = 1.5$, $w = 0.3$, $v_{\text{amp}} = 75$, $r_{\text{circ}} = 0.98$, $w_{\text{circ}} = 0.02$.

2.3. Boundary conditions

For the magnetic field we use perfect conductor boundary conditions both at the base of the convection zone (at $r = r_1$) and at the lateral boundary at the higher latitude ($\theta = \theta_1$). We assume the magnetic field to be antisymmetric about the equator ($\theta = \pi/2$), and at the outer radial boundary of the corona ($r = r_3$) we use the normal field condition. In terms of the magnetic vector potential $\overline{A} = (A_r, A_\theta, A_\phi)$, where $\overline{B} = \nabla \times \overline{A}$, these conditions become

$$\frac{\partial A_r}{\partial r} = A_\theta = A_\phi = 0 \quad (r = r_1), \tag{14}$$

$$A_r = 0, \quad \frac{\partial A_\theta}{\partial r} = -\frac{A_\theta}{r}, \quad \frac{\partial A_\phi}{\partial r} = -\frac{A_\phi}{r} \quad (r = r_3), \tag{15}$$

$$A_r = \frac{\partial A_\theta}{\partial\theta} = A_\phi = 0 \quad (\theta = \theta_1), \tag{16}$$

$$\frac{\partial A_r}{\partial\theta} = A_\theta = \frac{\partial}{\partial\theta}(\sin\theta A_\phi) = 0 \quad (\theta = \pi/2). \tag{17}$$
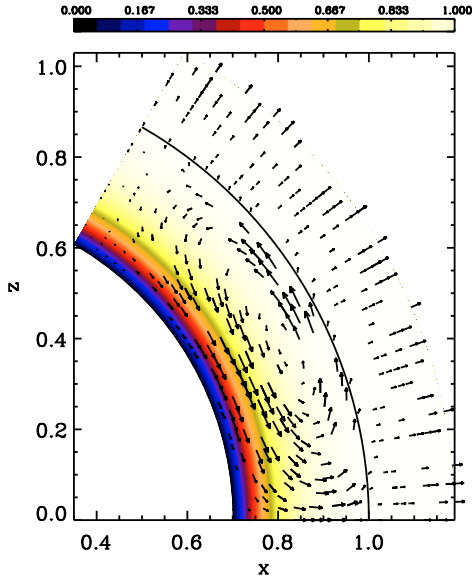
Fig. 1. Plot of the velocity field: the arrows show the meridional circulation and the wind, and the contours show the angular velocity. The solar radius is taken to be unity. Although our domain extends out to 5 solar radii, for clarity only a part of it is shown here. The curve at unit radius denotes the surface of the Sun.
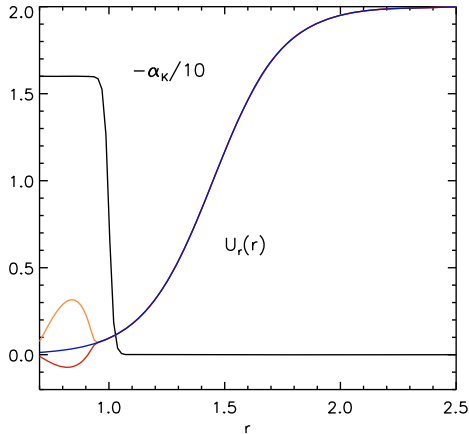

Fig. 2. The kinetic alpha effect, α_K, and wind radial velocity, U_r, as a function of radial coordinate r for three different latitudes, equator (*upper curve*), mid-latitude (*middle curve*) and latitude of upper boundary (*lower curve*). Note that the curves for the radial velocities differ only in $r < 1$, where the meridional circulation is non-zero.

For α_M, on those boundaries where the boundary condition on the magnetic field is "perfect-conductor" (i.e. at the bottom of the convection zone and at the higher latitude), we choose

$$\alpha_M = 0. \tag{18}$$

At the other two boundaries, we recall that since the PDE being solved is of first order in space we only need to specify one condition, which we have already imposed at the lower boundary. To calculate the derivative at the outer boundary we therefore just extrapolate the solution from inside to outside by a second order polynomial extrapolation. This is equivalent to using second order one sided finite difference at these boundaries.
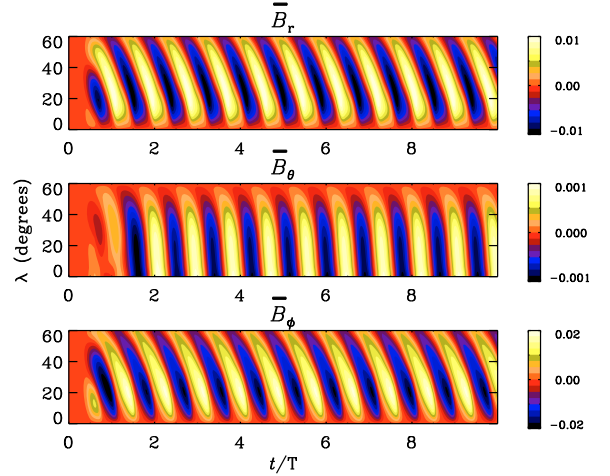

Fig. 3. Spacetime diagrams for the three components of the magnetic field. These plots are for the set of parameters corresponding to the velocity field and α_K shown in Figs. 1 and 2.

As the initial condition for the magnetic field we choose our seed magnetic vector potential from a random Gaussian distribution with no spatial correlation and root-mean-square value of the order of 10^{-4} times the equipartition field strength. Also, initially we take $\alpha_M = \alpha - \alpha_K = 0$.

3. Results

In order to demonstrate that our dynamo is excited, and displays both oscillations and equatorward migration, we first use the velocity field and the kinetic α profile shown in Fig. 1, with $Re_M = 3 \times 10^2$ and solve Eqs. (2) and (3) simultaneously. The resulting space-time diagram for the three components of the magnetic field is shown in Fig. 3. This is a typical example of the "butterfly" diagrams that are obtained with this model.

As mentioned above, an important feature of MF dynamos in the absence of wind and meridional circulation (i.e. when $U_0 = 0$ and $v_{amp} = 0$), is that they are severely quenched as Re_M increases. To show this we have plotted in Fig. 4a the time-series of the total magnetic energy $E_M = \frac{1}{2}\langle \overline{B}^2 \rangle$ for several values of Re_M. Here, $\langle ... \rangle$ denotes averaging over the domain $r_1 \leq r \leq r_2$. Clearly the total magnetic energy decreases with Re_M. Similar quenching, as a result of the dynamical evolution of the alpha term, has been seen in many different models of the solar dynamo (see, e.g., Chatterjee et al. 2010, 2011; Guerrero et al. 2010, for some recent examples), and also in models of galactic dynamos (Shukurov et al. 2006).

To substantiate this further we plot in Fig. 5 the time-averaged magnetic energy $\langle E_M \rangle_t$ as a function of Re_M, where the time averaging is done over several diffusion times (T) in the saturated nonlinear stage (i.e. after the kinematic growth phase is over). Time averaging is here indicated by the subscript t after the averaging sign. As can be seen in the absence of wind, i.e. with $U_0 = 0$, such time-averaged energy falls off approximately as Re_M^{-1}. This gives a quantitative measure of the quenching. (The point at $Re_M = 2 \times 10^6$ appears anomalous; we believe this is because we have not run the code for long enough to achieve the final saturated state.)

To demonstrate the ability of the wind and circulation to act together to alleviate quenching, we have plotted in Fig. 4(b) the time-series of E_M for several different values of Re_M, in the presence of the wind (with $U_0 = 1$, $v_{amp} = 75$ and depth parameter
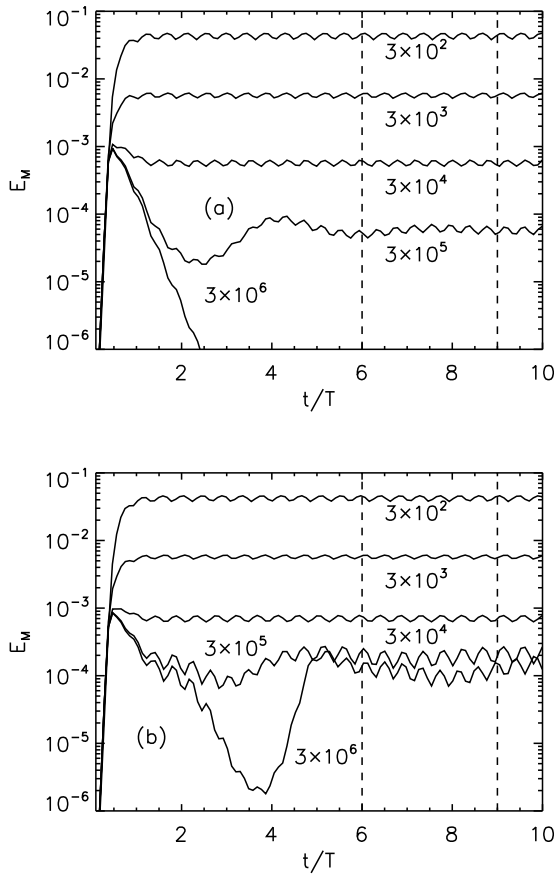
Fig. 4. a) Time series of E_M for $U_0 = 0$ and $v_{amp} = 0$, i.e. no wind or circulation, for 5 different values of Re_M. **b)** The corresponding plot with $U_0 = 1$, $w = 0.3$ and $v_{amp} = 75$. The time-averaged magnetic energy $\langle E_M \rangle_t$ is calculated by time-averaging these time-series between the two dashed vertical lines. The other parameters used are $\alpha_0 = 16$, $w_\alpha = 0.2$, $r_2 = 1.5$, and $w = 0.3$.

Fig. 5. The time-averaged magnetic energy as a function of Re_M for $U_0 = 0$ (no wind) and $U_0 = 1$ and $w = 0.3$ and $v_{amp} = 75$.

Fig. 6. Time series of E_M for 5 different values of U_0, namely, $U_0 = 0.1(*), 0.4(\diamond), 1(\triangle), 2(\square)$ and $10(\times)$ with all other parameters held fixed, in particular $Re_M = 10^7$, $w = 0.3$.

$w = 0.3$). The dependence of the time-averaged magnetic energy $\langle E_M \rangle_t$ on Re_M in this case is also plotted in Fig. 5. Comparing Fig. 4(b) with Fig. 4(a) and also comparing the two lines in Fig. 5 we clearly see that with the parameters chosen the wind in conjunction with the circulation is capable of alleviating quenching. This is one of our principal results. Note that the saturated mean field energy that we observe at large Re_M is still rather small, only slightly exceeding 10^{-4} of the equipartition value.

Next we attempt to isolate the role of each parameter in our model. First we make a detailed systematic study of how quenching depends on the two parameters U_0 and w of our model, for a fixed value of $Re_M = 10^7$ and zero circulation, $v_{amp} = 0$. For each pair of parameters we ran our code for up to 50 diffusion times. In some cases the time series of E_M declines as a function of time initially, but at larger times recovers to unquenched values, e.g. $U_0 = 1$ in Fig. 6. In some other cases we observe that the recovery is merely temporary and at large times E_M goes to zero. As an example we first show in Fig. 6 the time-series of E_M for various values of U_0, for a fixed $w = 0.3$. Clearly, as the wind velocity increases the transport of magnetic helicity out of the domain at first becomes more efficient and we observe less quenching. But this alleviation of quenching must have its limits because for a large enough wind speed the magnetic field itself will be advected out of the domain faster than it is generated, thus killing the dynamo (see, e.g., Shukurov et al. 2006;
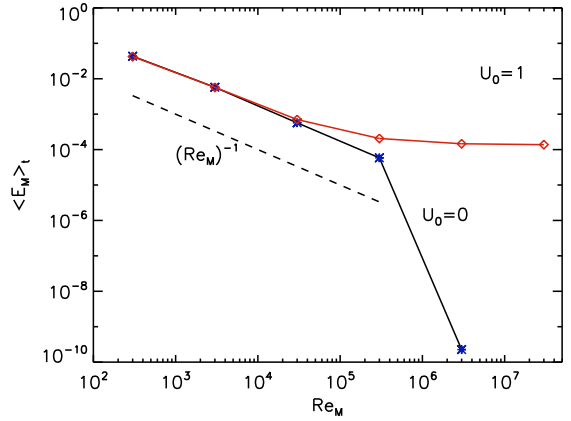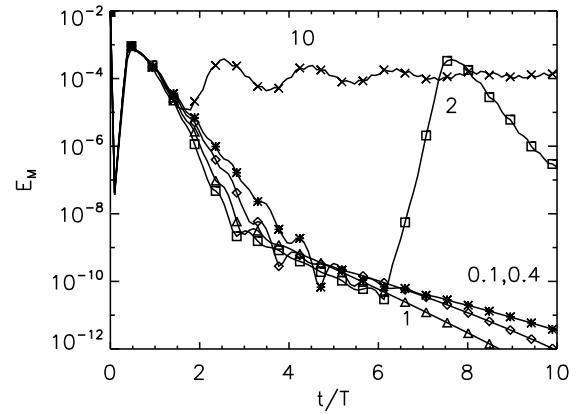
Brandenburg et al. 1993; Moss et al. 2010). However with penetration factor $w = 0.3$ we did not find this effect, even when $U_0 = 100$, but with $w = 0.5$, winds with $U_0 \geq 20$ kill the dynamo. We deduce that it is necessary to advect large-scale field from a substantial proportion of the dynamo region for the dynamo to be killed by advection.

Then we consider the parameter w which controls the depth of penetration of the wind into the convection zone. The dependence of the time-series of magnetic energy on this parameter is shown in Fig. 7, for $Re_M = 10^7$ and $U_0 = 2$. We also note that there is a subset of parameters for which the transients are so long that it is difficult to decide whether the asymptotic state is a quenched dynamo or not, within reasonable integration times. In our parameter space, i.e. in the $U_0 - w$ plane, the positions of the quenched and unquenched runs are shown in Fig. 8; summarizing the dependence of quenching on these parameters. For all the runs we label as unquenched the butterfly diagram is also restored at large times.

3.1. The effect of circulation

Next we consider the effect of meridional circulation on the quenching. If the wind penetrates inside the convection zone too deeply then we expect that circulation will have either no effect,
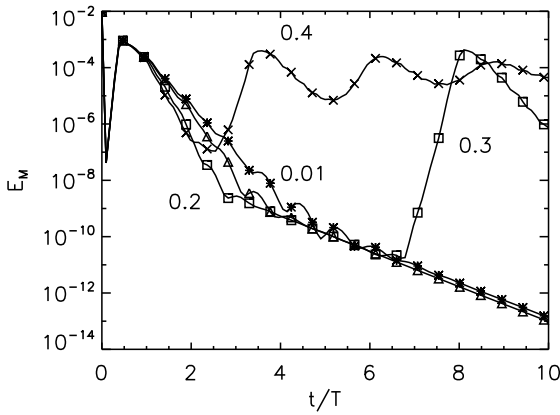
Fig. 7. Time series of E_M for 5 different values of w, [$w = 0.01(*)$, $0.2(\triangle)$, $0.3(\square)$, and $0.4(\times)$.] with all other parameters held fixed, i.e., $\mathrm{Re_M} = 10^7$, $U_0 = 2$ with no circulation.

Fig. 9. Time series of E_M as a function of time for $U_0 = 2$ and $w = 0.25$ with $v_{amp} = 0(+)$, $75(*)$, $100(\diamond)$, and $200(\triangle)$.
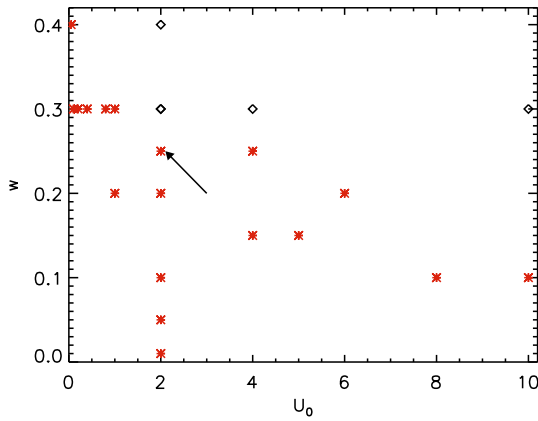

Fig. 8. The incidence of quenched and unquenched solutions in the $U_0 - w$ plane. The positions of quenched models are denoted by the symbol $*$, the symbol $\diamond$ identifies unquenched models. The arrow is explained in Sect. 3.1.

the term $\kappa_t \nabla^2 \alpha_M$ to the right hand side of Eq. (3), where κ_t is an effective turbulent diffusivity of the magnetic helicity. Numerical simulations have estimated $\kappa_t \sim 0.3\eta_t$ (Mitra et al. 2010a). We have checked that such a diffusive flux of magnetic helicity can alleviate quenching at least as effectively as the meridional circulation, in the presence of the wind.

Finally we note that the alleviation of quenching as described here is independent of some details of the underlying dynamo model. In particular it does not depend on whether we have an α^2 dynamo or an $\alpha^2\Omega$ dynamo. To check this assertion explicitly we also solved the same problem but with $U^{shear} = 0$ in Eq. (1). The results are shown in Fig. 10 where we compare the alleviation of quenching for the α^2 dynamo (top panel) against the corresponding $\alpha^2\Omega$ dynamo (bottom panel).

4. Conclusions

We have introduced two observationally motivated effects that may help reduce the catastrophic quenching found in mean field dynamo models. An outward flow from the dynamo region ("wind") is found to be effective in allowing the quenching to saturate at finite values of the field strength. The wind alone is, however, only effective when it penetrates quite deeply into the convection zone. These effects are modified to some extent by the presence of a meridional circulation which has the ability to transport small scale helicity from deep in the convection zone to near the surface, from where the wind can more effectively remove it. However, the effects of circulation in our model are not dramatic. It is also true that the saturation fields in our model are rather small compared to the equipartition field strength. This was also observed in the model of Shukurov et al. (2006); see also Moss & Sokoloff (2011). One possibility, that we have not explored, is that the neglected inhomogeneity of the solar convection zone may be important.

It is interesting to try to estimate the various parameters of our model in physical units and to compare them with the solar values. We have taken the solar radius as the unit of length (7×10^{10} cm). The α effect can be taken to be a measure of the small scale velocity in the Sun, $\alpha \sim (1/3)|\boldsymbol{u}|$, where $\boldsymbol{u} = \boldsymbol{U} - \overline{\boldsymbol{U}}$. The Baker & Temesvary (1966) tables give estimates for small-scale velocities in the convection zone of the Sun of between 4×10^3–2×10^5 cm s^{-1}, in regions where convection is efficient. As we have considered the convection zone to be homogeneous we consider 10^4 cm s^{-1} to be a reasonable estimate. Then, as

or just a marginal effect, because the wind by itself will be efficient enough in removing small-scale magnetic helicity from deep within the domain. But if the wind does not penetrate so deeply, circulation may play an important role in dredging magnetic helicity from deep inside the domain to near the surface from where the wind can remove it. To see whether this idea can work, we select one point in the phase diagram in Fig 8, where we obtain the quenched solution marked by the arrow. Then we turn on the meridional circulation. The comparison between the time-series of E_M with and without circulation is shown in Fig. 9. It can be seen that the final magnetic energy reached does not depend on the amplitude of circulation if the amplitude of circulation is greater than a critical value. Note that this alleviation of quenching by the circulation only works for those points in the $U_0 - w$ parameter space which lie close to the boundary between the quenched and non-quenched states in the phase diagram. For points with very small w, i.e. in cases where the wind penetrates very little into the convection zone, even a very strong circulation cannot remove the quenching.

Another possible mechanism that can transport magnetic helicity from the bulk of the convection zone to its surface is the diffusion of magnetic helicity. This can be described by adding
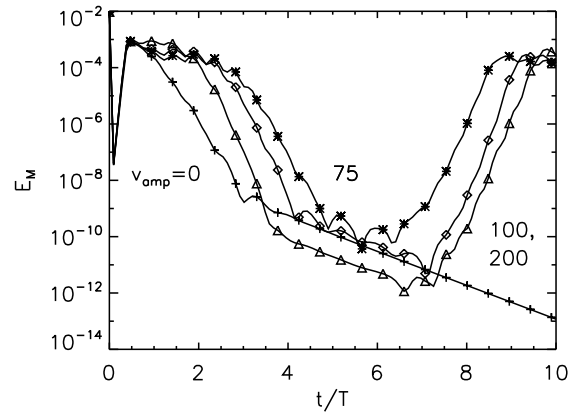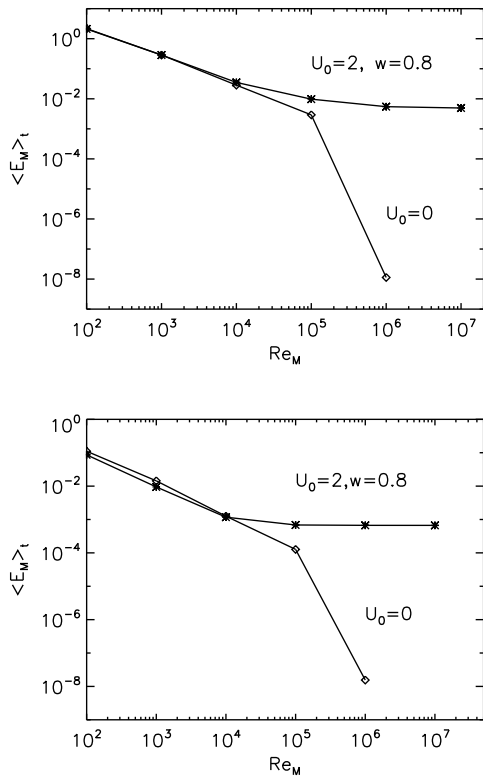
Fig. 10. The behaviour of the time-averaged magnetic energy as a function of magnetic Reynolds number Re_M, which shows the alleviation of quenching, with wind speed $U_0 = 2$ and depth parameter $w = 0.8$ (*upper panel*). Also shown is the corresponding plot in the absence of a wind, which clearly shows a catastrophic quenching. The *lower panel* is for a $\alpha^2\Omega$ dynamo.

$\alpha = 16$ in our units the unit of velocity is $\sim 10^4/(3 \times 16)$ cm s^{-1} $\sim 2 \times 10^3$ cm s^{-1}, and the unit of time, obtained from length and velocity units given above, is $\sim 10^8$ s ≈ 10 yrs. Thus our characteristic cycle period, $T \approx 1$, corresponds to approximately 10 years. Then the maximum wind speed we have used ($U_0 = 10$) would correspond to 2×10^3 cm s^{-1}. The speed of the meridional circulation at the surface in our units is $v_{surf} = 0.47$ for $v_{amp} = 75$. Translated to physical units this becomes $v_{surf} \approx 1$ m s^{-1}, which is of the same order of magnitude as the solar meridional velocity. If in the estimates above we use the maximum and minimum values of the small-scale velocity as given by the Baker and Temesvary tables, instead of the mean, the maximum surface speed of meridional circulation will be between 0.4 m s^{-1} and 20 m s^{-1} . The speed of the solar wind that we have used is significantly smaller than that of the actual solar wind, but on the other hand the real solar wind is a highly fluctuating turbulent flow, whereas we have considered a constant outflow.

To summarise, we have presented a very simplified model, in order to explore some basic ideas relevant to the solar dynamo.

We cannot claim to have "solved" the quenching problem, but feel we have identified, and to some extent quantified, mechanisms of potential interest. We appreciate that there are a number of desirable improvements, even in this MF formulation. These include using a more realistic solar-like rotation law, investigation and comparison of the effects of other fluxes of magnetic helicity (e.g. Zhang et al. 2006), the diffusive magnetic helicity flux (Mitra et al. 2010a), the inclusion of compressibility in some form, but most importantly perhaps, using a more realistic model for the solar wind allowing for magnetic helicity loading via coronal mass ejections. Notwithstanding these possible shortcomings, we do feel that our results provide motivation for further investigations in the context of solar and stellar dynamos. Investigations using DNS (e.g. Warnecke & Brandenburg 2010) appear likely to be especially interesting, and we hope to pursue this approach.

References

Baker, N. H., & Temesvary, S. 1966, Tables of Convective Stellar Envelopes (New York: Institute for Space Studies)
Blackman, E., & Field, G. B. 2000, ApJ, 534, 984
Blackman, E., & Brandenburg, A. 2002, ApJ, 579, 359
Blackman, E., & Brandenburg, A. 2003, ApJ, 584, L99
Brandenburg, A., & Käpylä, P. J. 2007, New. J. Phys., 9, 305
Brandenburg, A., & Sandin, C. 2004, A&A, 427, 13
Brandenburg, A., & Subramanian, K. 2005, Phys. Rep., 417, 1
Brandenburg, A., Donner, K.-J., Moss, D., et al. 1993, A&A, 271, 36
Brandenburg, A., Candelaresi, S., & Chatterjee, P. 2009, MNRAS, 398, 1414
Cattaneo, F., & Hughes, D. W. 1996, Phys. Rev. E, 54, 4532
Chatterjee, P., Brandenburg, A., & Guerrero, G. 2010, Geophys. Astrophys. Fluid Dyn., 104, 591
Chatterjee, P., Guerrero, G., & Brandenburg, A. 2011, A&A, 525, A5
Dikpati, M., & Gilman, P. A. 2009, Space Sci. Rev., 144, 67
Gruzinov, A. V., & Diamond, P. H. 1994, Phys. Rev. Lett., 72, 1651
Guerrero, G., Chatterjee, P., & Brandenburg, A. 2010, MNRAS, 409, 1619
Kleeorin, N., Moss, D., Rogachevskii, I., & Sokoloff, D. 2000, A&A, 361, L5
Käpylä, P. J., Korpi, M. J., Brandenburg, A., Mitra, D., & Tavakol, R. 2010, Astron. Nachr., 331, 73
Krause, F., & Rädler, K.-H. 1980, Mean-field Magnetohydrodynamics and Dynamo Theory (Oxford: Pergamon Press)
Mitra, D., Candelaresi, S., Chatterjee, P., Tavakol, R., & Brandenburg, A. 2010a, Astron. Nachr., 331, 130
Mitra, D., Tavakol, R., Käpylä, P. J., & Brandenburg, A. 2010b, ApJ, 719, L1
Moss, D., & Sokoloff, D. 2011, Astron. Nachr. 332, 88
Moss, D., Sokoloff, D., Beck, R., & Krause, M. 2010, A&A, 512, A61
Shukurov, A., Sokoloff, D., Subramanian, K., & Brandenburg, A. 2006, A&A, 448, L33
Subramanian, K., & Brandenburg, A. 2004, Phys. Rev. Lett., 93, 205001
Vainshtein, S. I., & Cattaneo, J. 1992, ApJ, 393, 165
Vishniac, E. T., & Cho, J. 2001, ApJ, 550, 752
Warnecke, J., & Brandenburg, A. 2010, A&A, 523, A19
Zeldovich, Ya. B, Ruzmaikin, A. A., & Sokoloff, D. D. 1983, Magnetic Fields in Astrophysics (New York: Gordon and Breach Science Publishers).
Zhang, H., Sokoloff, I., Rogachevskii, I., et al. 2006, MNRAS, 365, 276